Electronic structure of isolated aluminum point defects and associated trigonal pairs and clusters in Si

H. Overhof and H. Weihrich
Institut for Theoretical Physics, Physics Department, University of Paderborn, D 4790 Paderborn, Federal Republic of Germany

G. Corradi
Research Laboratory for Crystal Physics, Hungarian Academy of Sciences, H-1502 Budapest Pf. 132, Hungary
(Received 11 October 1991)

We use the self-consistent linear-muffin-tin-orbital method in the atomic-sphere approximation for the calculation of the electronic structure, total energies, and hyperfine fields for isolated Al point defects and for trigonal Al defect pairs in silicon. Many-body effects are treated in the local-density approximation of density-functional theory and the band gap appropriate for Si is obtained using the scissors-operator technique. We find that the substitutional Al_{Si} point defect is thermodynamically stable while the (Al_{Si}-Al_{Si}) pairs, the interstitial Al_i point defects, the (Al_i-Al_{Si}) pairs, and the (Al_i-Al_i) pairs are metastable. We calculate the hyperfine-interaction (HFI) matrix elements, the contact term, as well as the full dipolar tensor for the Al nuclei and for the first ligand shells. We discuss results obtained for several trigonal (Al_i-Al_{Si}) pairs which differ with respect to the distance between the two Al atoms. No pair was found that has the large hyperfine-interaction matrix element with the Al_{Si} nucleus, which is the characteristic of Si-G20. We have, therefore, calculated different clusters where in addition to the trigonal (Al_i-Al_{Si}) pair another Al_{Si} or C_{Si} constituent was built-in, thus preserving the trigonal symmetry. The search was unsuccessful, however.

I. INTRODUCTION

In thermal equilibrium aluminum is built-in into silicon as a substitutional shallow acceptor. Upon irradiation with electrons at lower temperatures Si self-interstitials are formed[1] which are mobile even at low temperatures. If a self-interstitial and a substitutional Al_{Si} point defect meet they can change places ("kick-out" mechanism[1]) producing Al_i interstitials. These have been observed first in the paramagnetic Al_i^{++} state as Si-G18 by Watkins.[1] At elevated temperatures the Al_i interstitials become mobile, move to residual Al_{Si} point defects and form defect associates. Two such defects, Si-G19 and Si-G20, both with trigonal symmetry, each containing an interstitial and a substitutional Al atom, have been observed by Watkins.[1] These defects are interesting since atoms of the same chemical species are built into the lattice at two nonequivalent lattice positions. The two defect atoms have grossly different formal charge states and quite different properties as, e.g., spin density and electronic configuration.

Spin densities at the Al nuclei determined experimentally by electron paramagnetic resonance (EPR) both for isolated point defects and trigonal defect pairs have been published by Watkins.[1] A detailed investigation of the hyperfine interaction (HFI) with the ^{29}Si ligands has been performed by Brower[2] for Si-G18 and in more detail by Niklas, Spaeth, and Watkins[3] for Si-G18 and Si-G19 using the electron-nuclear double resonance (ENDOR) technique. These HFI data present precise information about the spin density at the different impurity and ligand and nuclear sites. The experimental methods, however, can at most determine the direction of the distance vector from the impurity center to the ligand nucleus. The length of this distance vector cannot be determined directly. The assignment of experimental data to the neighbor shells is therefore not possible on the basis of experimental data alone.

Theoretical total-energy calculations present powerful tools to investigate whether a defect configuration is stable or metastable, which pairs can be formed, etc. From these calculations in addition the HFI matrix elements can be obtained which can be compared directly with EPR and ENDOR data. It is the aim of this paper to investigate theoretically the isolated Al point defects and several trigonal defect pairs involving two different Al atoms. We also calculate theoretically the HFI matrix elements for these defects, both at the Al nuclei and at the Si ligands. We succeed in identifying the pair configuration corresponding to Si-G19. We do *not* find, however, a pair which has the large contact HFI at the Al_{Si} nucleus as that reported for Si-G20. Preliminary calculations for trigonal triple-defect complexes involving three Al atoms and for trigonal complexes involving two Al and one C atom as suggested by Watkins[4] have also been unsuccessful with respect to a possible identification of Si-G20.

It has been claimed[3] that the comparison of experimental HFI data for a highly symmetrical defect such as the tetrahedral Al_i point defect with data for a distorted defect like the (Al_i-Al_{Si}) pair makes a definite assignment possible. We shall show that the ambiguities inherent in all attempts to assign experimental HFI data to ligand shells in the case of a tetrahedral point defect cannot be

overcome by a comparison with HFI data for the pair. We show that a very good agreement of HFI data calculated theoretically from first principles with experimental data for Si-G18 and Si-G19 is obtained. The results show that the assignment proposed in Ref. 3 must be modified: the first two ⟨111⟩ Si ligand shells must be interchanged as was already considered by Brower[2] for the isolated defect Si-G18. Our new assignment is supported by the general shape of the spin-density distribution of the defect-induced state in the gap for both systems.

II. COMPUTATIONAL

Our calculations have been performed within the general framework of the spin-density functional theory (DFT). Exchange and correlation are treated in the local spin-density approximation (LSDA) of the spin-density functional theory.

For the computations we have made use of the self-consistent linear-muffin-tin-orbital method in the atomic-sphere approximation[5] (LMTO-ASA). In this method the crystal is divided into (overlapping) spheres in which the potential is assumed to be spherically symmetrical. A self-consistent solution for the perfect crystal and the corresponding Green function G_0 is calculated. Next it is assumed that the presence of the defect changes the LSDA potential in a small region around the defect only and for this "perturbed region" a Dyson equation for the perturbed Green function is solved self-consistently using G_0 with the potential ΔV which is the difference between the potential of a crystal with a defect and that of the perfect crystal. The LMTO method allows the calculation of the wave functions in the region near the nuclei which dominates the contributions to the HFI matrix elements. The use of the ASA unfortunately prohibits the introduction of any lattice relaxation effects.

Since the computational effort rises drastically with the size of the perturbed region the self-consistent calculation was limited to a rather small perturbed region. For the case of the isolated interstitial Al_i point defect the perturbed region contained the point defect, the four nearest-neighbor Si ligands and the six next-nearest-neighbor Si ligands. It also contained 14 "empty" ASA spheres introduced to fill the open structure of the diamond lattice. The potential ΔV obtained from a self-consistent solution of the Dyson equation for this rather small perturbed region was then used to solve the Dyson equation non-self-consistently for perturbed regions that also contained Si ligands located in more distant shells. In that way it was possible to calculate the HFI matrix elements for eight shells of neighbors in the case of isolated Al_i^{++} point defects and for 11 shells for the pairs. By a shell we denote all the atoms that are transformed into each other by the point-group symmetry operations of the crystal with the defect. We shall in the following list only one member of a shell by the distance vector from the Al_i^{++} to this ligand in units of $d/4$ where d is the lattice constant.

The small size of the perturbed region presents difficulties if one attempts to calculate the pair formation energies, in particular for more distant pairs. The pair formation energy is the difference between the total energy of the pair and the sum of the total energies of the constituents of the pair as isolated defects. Since the pair formation energy is always the small difference of large energies we have to take precautions that the different geometries of the perturbed regions for the different pairs do not influence the results. To this aim we have calculated the total energies of the constituents for a given pair with the same geometry for the perturbed region used for the pair: for the trigonal Al_i-Al_{Si} pair, e.g., we determine the total energy of the Al_i^{++} constituent from a total energy calculation for a trigonal pair where the Al_{Si}^{-} is replaced by Si, etc. Using this rather time-consuming procedure the pair formation energies of the very distant pairs turned out to be reasonably small in all cases.

It is well known that the single-particle band gap of the DFT-LSDA is too small by about 0.5 eV if compared to the experimental band gap. In previous calculations[6–8] on chalcogen in Si this small gap resulted in a shift of the defect-induced gap state into the bottom of the conduction band where it forms a resonance. In the case of Al_i we use the scissors-operator technique described by Beeler and co-workers[9,10] in order to ensure that the defect-induced state has its single-particle energy in the fundamental band gap. Without the use of the scissors operator which gives the experimental band gap for the crystal this defect state would be found in the valence band where it would be diamagnetic. Alternatively we have calculated the HFI for the paramagnetic defects and defect pairs in a *non-self-consistent* manner without the use of a scissors operator. Instead we used an extra square well potential for the perturbed region that moves the defect state into the band gap. We have found very little differences (less than 10% for the contact HFI at the Al_i^{++} nucleus) between both calculations. As in the case of the chalcogen substitutional defects in Si (Refs. 6–8) we find that the wave function of a deep state is not dramatically affected by a change of the potential even if the single-particle state is moved from the band edge to the center of the band gap.

The hyperfine interactions for our systems are relatively simple because we deal with $S = \frac{1}{2}$ orbital singlet states. In this case the isotropic hyperfine interaction for an electron with g factor g_e interacting with a nucleus at the site $\mathbf{R}_N$ with g factor g_N is given by

$$a_N = \tfrac{2}{3}\,\mu_0\, g_e\, g_N\, \mu_N\, m(\mathbf{R}_N), \tag{1}$$

where μ_0 is the susceptibility constant and μ_N is the nuclear magneton. The magnetization density $m(\mathbf{R}_N)$ at the nuclear site $\mathbf{R}_N$ is the product of Bohr's magneton μ_B, and the difference $m(\mathbf{r})$ between the electron spin densities of up and down spins, $n_\uparrow$ and $n_\downarrow$, respectively

$$m(\mathbf{r}) = \mu_B\,[n_\uparrow(\mathbf{r}) - n_\downarrow(\mathbf{r})]. \tag{2}$$

$m(\mathbf{r})$ will be analyzed in terms of three different contributions. The first contribution arises from the paramagnetic spin of the single-particle state in the gap. This contribution actuates the magnetization of other states leading to a spin polarization of the valence states, and

also to a spin polarization of the impurity and ligand core states.

The anisotropic (dipolar) HFI is given by an integral over the magnetization density over all space

$$(b_N)_{i,j} = \frac{\mu_0}{8\pi} g_e g_N \mu_N \int \frac{3x_i x_j - r^2\delta_{i,j}}{r^5} m(\mathbf{r}+\mathbf{R}_N)\, d^3r. \tag{3}$$

The integrand is strongly peaked at the nucleus and, therefore, it is sufficient in practically all cases to perform the integration over the central ASA sphere. The contributions from the other spheres can be approximated replacing the spin distribution in each of these spheres by point dipoles with a dipole moment appropriate for the integrated spin density in the spheres. The anisotropic hyperfine tensor can be diagonalized and cast into the form

$$(b_N)_{i,j} = \begin{pmatrix} -b+b' & 0 & 0 \\ 0 & -b-b' & 0 \\ 0 & 0 & 2b \end{pmatrix}. \tag{4}$$

If the spin density has axial symmetry the dipolar constant b' must be zero. For nuclei that are not located on at least a threefold-symmetry axis of the perturbed region, b' will in general be nonzero. The principal z axis of each calculated HFI tensor is by symmetry in the (110) plane [our calculations do not include ligands that are outside the (110) plane]. We shall give the orientation of the principal axis in this plane with respect to the direction from the Al_i^{++} to the ligand.

For the hyperfine matrix elements a_N and b_N we shall give the correct signs. Most of the calculated HFI data for Si ligands will therefore be negative because the g factor g_N for ^{29}Si is negative. This is in contrast to our earlier papers.[8,11] From magnetic resonance experiments the absolute signs of the HFI matrix elements usually are not determined; however, it is possible to determine the relative signs of b_N with respect to a_N. We shall indicate this sign ambiguity using $\pm$ and $\mp$ as signs.

In the following we denote by a_l and b_l the hyperfine matrix elements which are calculated from the spin density of the single-particle spin density of the deep state alone. By $a_{\rm tot}$ and $b_{\rm tot}$ we denote the hyperfine matrix elements which are calculated from the total spin densities which includes contributions from the deep state, the valence band, and from the core states. The spin polarization of the core states was taken into account in each step of the self-consistent cycle using the potential derived from the solution of Dyson's equation in an atomic Dirac-LSDA calculation. For the more distant ligands for which no self-consistent calculation of the spin density was possible the core polarization has not been determined.

III. ISOLATED Al POINT DEFECTS

We have calculated the total energies for isolated Al point defects located at the tetrahedral interstitial and substitutional sites. For Al_{Si} we can obtain the negative charge state Al_{Si}^- only. There is no state in the gap for Al_{Si}^- but a resonance at the valence-band edge which transforms according to the T_2 irreducible representation. The neutral charge state, Al_{Si}^0, is known to be a shallow state which extends over many unit cells and, therefore, cannot be computed by our methods.

For p-type Si the total energy of an isolated Al point defect in an interstitial position turns out to be by about 4 eV larger than that of an Al point defect in a substitutional position. We thus do not expect to find Al interstitials in thermal equilibrium. If Si self-interstitials are present, the reaction

$$Si_i^{++} + Al_{Si}^- \rightarrow Si_{Si} + Al_i^{++} + \Delta E + e(E_F - E_V)$$

can take place. Since $\Delta E = 2$ eV according to our total energy calculation the reaction will transform Al_{Si} into Al_i for all positions of the Fermi energy E_F with respect to the valence-band edge E_V. For the interstitial Al_i point defect we find two different charge states, Al_i^{++} and Al_i^+, with a removal energy $E^{++/+} = E_V + 0.58$ eV which must be compared with the value $E^{++/+} = E_V + 0.17$ obtained experimentally.[12] The agreement is not too convincing due to the fact that we have used a scissors operator. According to our calculations there is no neutral state for Al_i as, e.g., postulated by Troxell *et al.*[12] However, we find a resonance transforming according to the T_2 irreducible representation at the bottom of the conduction band. This state must be subject to a Jahn-Teller distortion which can significantly lower its energy. This result is in general agreement with the prediction of Troxell *et al.* that Al_i in the neutral state is accompanied by a significant lattice relaxation.

The single-particle wave function of the a_1 state in the gap listed in Table I is quite different from the corresponding wave functions of the deep levels of, e.g., substitutional chalcogen in Si: about 15% of the particle density is found in the Al ASA sphere compared to only 4% in the case of S_{Si}. In Fig. 1 we show a contour plot

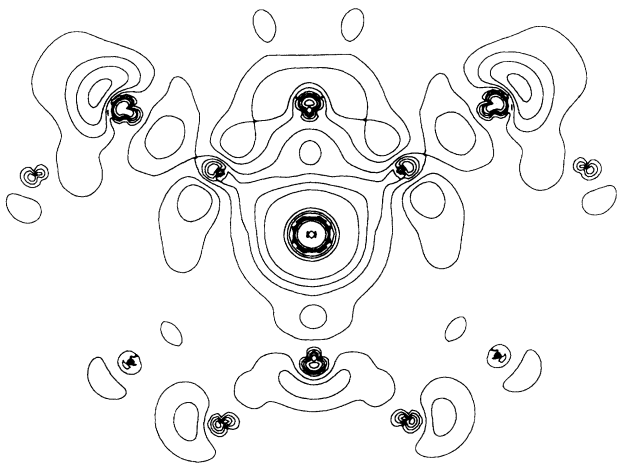

FIG. 1. Contour plot of the particle density for the gap state of Al_i^{++} in the (110) plane. The Al atom is at the center of the figure, the Si ligands can be identified from the oscillations of the particle density in the core regions.

TABLE I. Occupation of the different partial waves for the Al_i^{++} and the $(Al_i\text{-}Al_{Si})^+$ pair [pair (a)].

Al_i^{++}					$(Al_i\text{-}Al_{Si})^+$				
Ligand	*s*	*p*	*d*	Total	Ligand	*s*	*p*	*d*	Total
$Al_i^{++}(0,0,0)$	0.1513	0.0	0.0	0.1513	$Al_i^{++}(0,0,0)$	0.1417	0.0	0.0	0.1417
					$Al_{Si}^{-}(1,1,1)$	0.0044	0.0021	0.0153	0.0218
Si(1,1,1)	0.0060	0.0013	0.0210	0.0283					
					$Si(1,\bar{1},\bar{1})$	0.0059	0.0003	0.0206	0.0268
					Si(2,0,0)	0.0047	0.0113	0.0040	0.0200
Si(2,0,0)	0.0038	0.0110	0.0049	0.0197					
					$Si(\bar{2},0,0)$	0.0042	0.0097	0.0058	0.0197
$Si(\bar{3},1,1)$	0.0005	0.0049	0.0012	0.0066	$Si(\bar{3},1,1)$	0.0005	0.0049	0.0012	0.0066
					Si(2,2,2)	0.0054	0.0200	0.0001	0.0255
Si(2,2,2)	0.0063	0.0256	0.0001	0.0319					
					$Si(2,\bar{2},\bar{2})$	0.0062	0.0243	0.0000	0.0305
$Si(\bar{2},\bar{2},\bar{2})$	0.0016	0.0003	0.0001	0.0020	$Si(\bar{2},\bar{2},\bar{2})$	0.0016	0.0001	0.0002	0.0019
					Si(3,3,1)	0.0000	0.0010	0.0017	0.0027
Si(3,3,1)	0.0001	0.0027	0.0009	0.0037					
					$Si(\bar{3},\bar{3},1)$	0.0001	0.0026	0.0009	0.0036
$Si(\bar{3},\bar{3},\bar{3})$	0.0000	0.0008	0.0001	0.0009					

of the particle density of the gap state of Al_i^{++} in the (110) plane. We see that the state in the gap is bonding and that the bond charges extending to the nearest neighbors in the ⟨111⟩ directions extend to the (2,2,2) ligands. This is possible since the wave function is predominantly *s*- and *d*-like at the (1,1,1) ligands whereas it is *s*- and *p*-like at the (2,2,2) ligands. Here the bond is terminated and there is about one order of magnitude less spin density at the (3,3,1) ligands compared to the (2,2,2) ligands. There is also a strong bond directed toward the next-nearest neighbors in the ⟨100⟩ directions and again the gap state essentially does not extend further. We thus have the picture that the interstitial Al_i^{++} ion is bound to the Si ligands whereby the bond charges extend as long as there is a straight chain of ligands. There is very little spin density extending toward the $\langle \bar{1}\,\bar{1}\,\bar{1} \rangle$ directions where the first ligands are farther apart. Except for the oscillations of the wave function within the core regions (we show in Fig. 1 the true wave function, not a pseudofunction) the wave function has no node within the rectangle spanned by the shell of (2,2,2) Si ligands. The wave function changes sign outside this rectangle where its magnitude is small, however, since already 75% of the gap state density is contained in the region covered by our calculation.

A comparison of the calculated HFI data with EPR and ENDOR data of Brower[2] and with ENDOR data by Niklas, Spaeth, and Watkins[3] directly reflects the results just discussed for the wave function of the gap state. As is evident from Table II the HFI at the defect nuclei and at all ligands is predominantly given by a_l which is the contribution of the gap state. Contributions from the valence-band polarization caused by the spin of the gap state are of relative significance only at ligands where a_l is very small. This is in contrast to the results for the chalcogen (substitutional) defects in Si (Refs. 6–8) where the polarization of the valence band was largest at ligands with larger contributions of the gap state to the contact HFI.

When comparing our data with experimental data of Niklas, Spaeth, and Watkins[3] we have interchanged the experimental data for the Si(1,1,1) and the Si(2,2,2) ligands, respectively. Brower[2] already noted that it is difficult to distinguish between the two shells from the magnetic resonance data alone. Both shells have approximately the same contact HFI while the dipolar HFI differ by nearly one order of magnitude. The reason for this can be seen if we compare wave functions of the gap state for both ligands: Since the wave function at the nearest neighbors is predominantly *d*-like there will be a small dipolar HFI matrix element whereas at the Si(2,2,2) ligand the wave function is mainly *p*-type and accordingly the dipolar HFI is much larger. The negative sign of b_{expt} with respect to a_{expt} observed experimentally for the ligand shell which we assign to Si(1,1,1) can be taken as an indication that the wave function has a strong *d* admixture as has been shown by van Wezep *et al.*[13] Our calculation gives the relatively small absolute value but does not give the correct sign in this case which, however, is the only sign inconsistency. We find a near-perfect

TABLE II. Comparison of the calculated and experimental hyperfine data for the isolated Al_i^{++} point defect (in MHz). a_l and b_l are calculated from the single-particle wave function of the state in the gap, a_{vb} and a_c are the contributions from the polarization of the valence-band and core states while a_{tot} and b_{tot} are the sum of all contributions. A dash means that a_c could not be calculated while missing data entries for b and b' represent a zero by symmetry. The experimental hyperfine interactions listed as a_{expt}, b_{expt}, and b'_{expt}, respectively, are taken from Brower (Ref. 2) for the interaction with the $^{27}Al_i^{++}$ nucleus and from Niklas, Spaeth, and Watkins (Ref. 3) for the interaction with the ^{29}Si ligands.

Ligand	a_l	a_{vb}	a_c	a_{tot}	a_{expt}	Tensor $axis_{theor}$	b_l	b_{tot}	b'	b_{expt}	b'_{expt}	Tensor $axis_{expt}$
Al_i^{++}	1287	70	8.0	1365	±1320							
Si(1,1,1)	-51.3	-3.4	0.2	-54.7	±50.09	[111]	-0.34	-0.68		∓0.05		[111]
Si(2,0,0)	-32.6	-0.5	0.4	-32.8	±22.6	[100]	-2.3	-2.3	0.07	±1.44	≃ 0	[100]
Si(3,1,1)	-3.92	0.53	—	-3.39	±3.51	[110]-19°	-1.05	-1.02	0.03	±0.89	∓0.04	[110]-15°
Si(2,2,2)	-51.4	-0.2	—	-51.6	±52.31	[111]	-5.62	-5.75		±3.91		[111]
Si($\bar{2},\bar{2},\bar{2}$)	-13.4	0.44	—	-12.92	±11.31	[111]	-0.06	-0.09		±0.16		[111]
Si(3,3,1)	-1.11	0.05	—	-1.06	±1.24	[110]+26°	- 0.56	-0.58	0.04	±0.16	±0.02	[110]-58°
Si($\bar{3},\bar{3},\bar{3}$)	-0.20	0.08	—	-0.11	±2.03 ?	[111]	≃ 0	≃ 0		±0.21 ?		[111]

agreement for the contact HFI matrix elements except for the Si(2,0,0) ligand for which the theoretical contact HFI is 44% larger than the experimental value. For the anisotropic HFI matrix elements the deviations generally are somewhat larger than for the contact HFI.

As in the case of chalcogens in Si (Ref. 8) we find that the spin density is neither isotropic nor a monotonous function of the distance from the paramagnetic defect: This is illustrated best by the HFI at Si($\bar{2},\bar{2},\bar{2}$) which is completely different from that at Si(2,2,2). In addition, the HFI matrix elements for Si($\bar{3}$,1,1) are much smaller in magnitude than those for Si(2,2,2) which is farther apart. We see from our data that the spin density of the isolated Al_i^{++} point defect is essentially contained in a small cluster containing the Al atom, its 14 neighbors in the (1,1,1), (2,2,2), and (2,0,0) shells. The ligands which are farther apart or which are in other directions with respect to the Al_i^{++} ion contribute little to the spin density.

IV. TRIGONAL Al-Al PAIRS

The stability of trigonal aluminum pairs with respect to dissociation is investigated by means of total-energy calculations for several trigonal pair configurations involving two Al atoms.

For the $(Al_{Si}\text{-}Al_{Si})^{--}$ pair where both Al atoms are at the nearest-neighbor position we find that the total energy of the pair is larger than the total energy of two isolated Al_{Si}^{-} point defects and hence is unstable. The pair formation energy is 1.2 eV for n-type samples which is more than the screened Coulomb repulsion of the two negatively charged Al ions. This is not unexpected since in addition the filled valence shells repel each other. The pair has two deep levels, the $E^{0/-}$ level at $E_V + 0.2$ eV and the $E^{-/--}$ level at $E_V + 0.48$ eV. If the Fermi level is at the valence-band edge these (antibonding) states are unoccupied. Accordingly the total energy of the pair in the neutral state is only about 0.4 eV higher than the total energy of two isolated Al_{Si} point defects. This pair, therefore, could be stable, in particular if stabilized by lattice relaxation. If the state in the gap is singly occupied it will be paramagnetic and predominantly p-type. It can be characterized by contact HFI of $a = 57.6$ and -3.6 MHz for the interactions at the ^{27}Al and the nearest-neighbor ^{29}Si nuclei, respectively, and by anisotropic HFI constants that amount to 30.65 and −2.088 MHz, respectively. Trigonal (Al_{Si}-Al_{Si}) pairs with a larger separation of the Al atoms (three nearest-neighbor distances at least) have total energies which according to our calculations cannot be distinguished from the total energy of two isolated Al_{Si} point defects.

The $(Al_i\text{-}Al_i)^{n+}$ pair where both Al atoms are located on nearest-neighbor tetrahedral interstitial positions is not stable with respect to pair dissociation. We find that the pair formation energy is about 0.7 eV for all charge states of the pair. We find a gap state at $E_V + 0.5$ eV which is antibonding. If this state is fully occupied the energy of the $(Al_i\text{-}Al_i)^{++}$ pair is 0.8 eV larger than twice the total energy of an isolated Al_i^{+} point defect. This slightly exceeds the screened Coulomb interaction of the pair (0.5 eV). If the state is unoccupied the much larger Coulomb interaction of the $(Al_i\text{-}Al_i)^{4+}$ pair is reduced by the occupied bonding configuration which is a resonance in the valence band. The total energy of the pair is still 0.7 eV larger than the corresponding value of isolated Al interstitials and, therefore, pair formation is unlikely.

Experimentally one finds two pairs which are trigo-

nal and involve two Al atoms, one of which is located on an interstitial position while the other substitutionally replaces one Si atom. The most extensively studied pair is Si-G19, identified as the $(Al_i\text{-}Al_{Si})$ pair by Watkins[1] which exists in the $(Al_i\text{-}Al_{Si})^+$ paramagnetic charge state. This state is also referred to as $Al_i^{++}\text{-}Al_{Si}^-$ in order to emphasize that the two Al atoms are differently charged. Since there is another paramagnetic trigonal $(Al_i\text{-}Al_{Si})^+$ pair reported in the literature [Si-G20, (Ref. 1)] we have performed total-energy calculations for several trigonal $(Al_i\text{-}Al_{Si})$ pair configurations which differ with respect to the distances between the Al atoms. These configurations are schematically shown in Fig. 2. Our results for the total energies of the pairs are summarized in Fig. 3. We find that for all positions of the Fermi energy the most stable pair is that for which the two Al atoms are separated by one nearest-neighbor distance. The pair formation energy of this pair is about −0.7 eV. The pair formation energies for the other pairs in the positively charged state are only slightly negative and therefore the stability of these pairs is questionable. For the neutral pair the picture changes significantly: the total energies of pairs (a) and (b) are virtually equal and also pair (c) appears to be stable. Obviously the larger distance of the defects in pair (b) with respect to pair (a) does not alter the binding energy of the pair because a Si atom is situated in between the defects. A similar result was obtained recently for the $(Fe_i\text{-}Al_{Si})^0$ pair.[14] For pair (c) an empty tetrahedral space separates the two constituents which significantly lowers the pair binding energy whereas pair (d) is quite similar to a dissociated pair.

We shall concentrate our discussion of the paramagnetic properties on pair (a) which will be identified with Si-G19. For this pair the calculated transition energy is $E^{+/0} = E_V + 0.7$ eV. A contour plot of the electron density of the gap state for this pair in the (110) plane is shown in Fig. 4. The particle density for the pair is remarkably similar to that of the isolated Al_i^{++} point defect with the exception that the negatively charged Al_{Si}^- is less attractive for electrons than the Si ligand which it

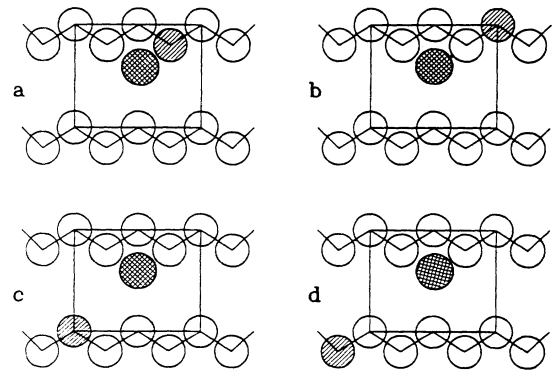

FIG. 2. Schematic representations of the different configurations of trigonal $Al_i\text{-}Al_{Si}$ pairs in Si in the (110) plane. Hatched balls represent Al_{Si}, cross line hatched circles represent Al_i, and plain circles represent Si atoms.

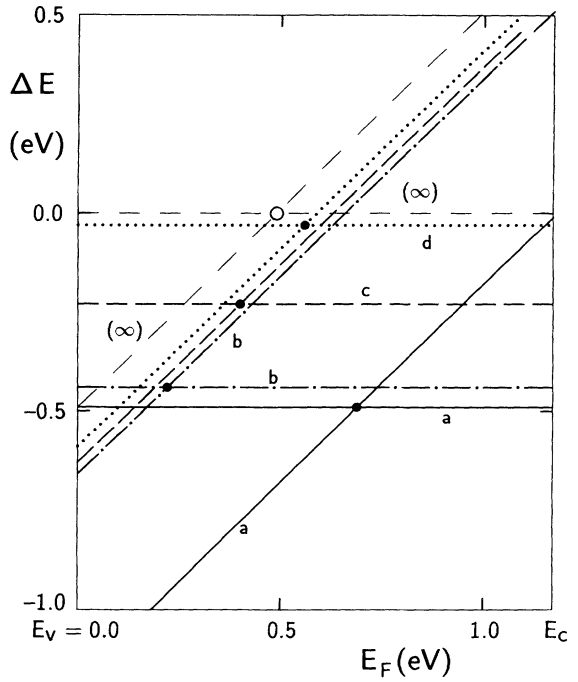

FIG. 3. Pair formation energy for the $(Al_i\text{-}Al_{Si})^{(n)}$ pairs in different atomic positions for the charge states (n) as a function of the Fermi energy. Lines with positive slope correspond to $n = 1$, lines with zero slopes represent neutral pairs. Full lines, dash-dotted lines, dashed lines, and dotted lines correspond to pair configurations (a), (b), (c), and (d), respectively, while thin dashed lines correspond to dissociated pairs. Circles mark electron removal energies.

replaces. This leads to the asymmetry of the particle density. We see that the pair formation is essentially caused by electrostatic forces and not by covalency. A quantitative comparison of the wave function for the gap state of the pair with that of isolated Al_i^{++} can be made with the help of Table I. For the comparison we must bear in mind

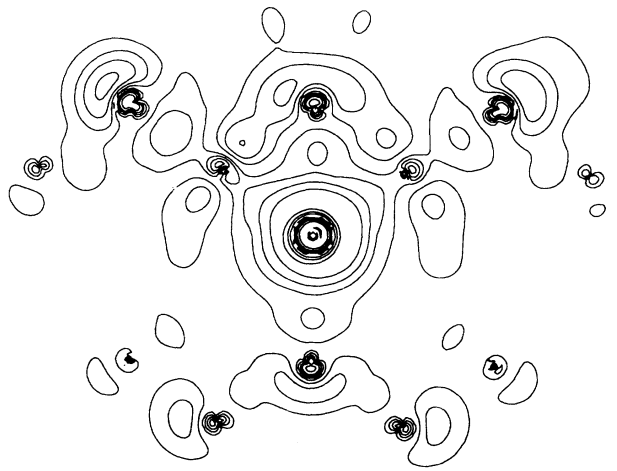

FIG. 4. Contour plot of the particle density for the gap state of the trigonal $(Al_i\text{-}Al_{Si})^+$ pair (a) in the (110) plane. The Al_i atom is at the center of the figure and the Al_{Si} is at (1,1,1) as can be seen from the slightly smaller particle density in this region.

that ligands which for the isolated point defect belong to the same shell now can become inequivalent due to the lower symmetry of the pair with respect to the isolated point defect. From the comparison of the data in Table I we see that the replacement of a Si atom by Al has no dramatic effect on the wave function: the occupancy of the Al_i^{++} s partial wave is reduced by 10%; the relative changes at the ligands are somewhat larger but the overall particle density distribution is not affected by the pair formation.

This insensitivity is also borne out by the HFI matrix elements listed in Table III. The agreement of our calculated data with the experimental results of Niklas, Spaeth, and Watkins[3] for the pair is remarkably good though somewhat inferior to the case of the isolated point defect. In particular the anisotropy introduced by the additional Al_{Si} is consistently underestimated by our calculation. The agreement of experimental dipolar HFI data with the experimental data is rather poor unless we interchange the assignment of the experimental data to the $Si(1,\bar{1},\bar{1})$ and the $Si(2,\bar{2},\bar{2})$ ligands. As in the case of isolated Al_i^{++} point defects the larger b_{ext} value belongs to the more distant ligand because here the wave function is s- and p-type whereas at the nearest-neighbor ligand the s and d character predominates.

Niklas, Spaeth, and Watkins[3] give the following argument for their assignment of ligand shells: they start from the observation that the quadrupole interaction constant requires that the two Al atoms are nearest neighbors. Since the HFI data for the pair are similar to those of the isolated point defect the replacement of the Si ligand by Al is regarded as a small trigonal perturbation of the HFI data except for the HFI interaction with the Al_{Si} nucleus itself. A small trigonal perturbation will split a $\langle 111\rangle$ ligand shell into a subshell of three ligands and a subshell containing just the ligand on the trigonal axis. If the perturbation is small enough it is possible from the HFI data to identify those two $\langle 111\rangle$ ligand subshells that belong to the same shell. However, there is one subshell with three $\langle 111\rangle$ ligands for which there is no corresponding subshell with one Si ligand because it is replaced by Al. This Si subshell must then be the one nearest to Al_i which in turn identifies the nearest Si shell for the isolated point defect.

The procedure is straightforward provided the difference between the HFI data for the different $\langle 111\rangle$ shells of the isolated Al_i point defect is much larger than the splitting between subshells introduced by the Al_{Si}. This is unfortunately not the case for the Al pair and hence the assignment of the data from the experiment alone is still ambiguous, in fact the choice made was wrong.

It remains to show that the pair Si-G19 observed experimentally can in fact be identified with our pair (a). An experimental hint is the quadrupolar interaction which is about a factor of 2 larger than one would expect for pair (a). For the other pairs the discrepancy would be much larger. Since for this interaction there is no valid theory (see, e.g., Lannoo[15]) the discrepancy might not be a strong argument. According to our total-energy calculations pair (a) is more strongly bound than pair (b) in the positive charge state, which need not be, however, the actual charge state at the diffusion temperature. A decision is not easy on the basis of the calculated HFI with the ^{27}Al nuclei for the different pairs listed in Table IV: The HFI contact interactions with the Al_i^{++} nucleus for all pairs are practically identical. The differences are much larger for the HFI interactions with the Al_{Si} nuclei which rules out pairs (c) and (d). The pairs (a) and (b) have about the same contact interactions and the calculated dipolar HFI data differ by a factor of 2 only

TABLE III. Comparison of the calculated and experimental hyperfine data for the trigonal $(Al_i\text{-}Al_{Si})^+$ defect pair [pair (a), in MHz]. a_l and b_l are calculated from the single-particle wave function of the state in the gap, a_{vb} and a_c are the contributions from the polarization of the valence-band and core states while a_{tot} and b_{tot} are the sum of all contributions. The experimental HFI interactions listed as a_{expt}, b_{expt}, and b'_{expt}, respectively, are taken from Watkins (Ref. 1) for the interaction with the ^{27}Al nucleus and from Niklas, Spaeth, and Watkins (Ref. 3) for the interaction with the ^{29}Si ligands.

Ligand	a_l	a_{vb}	a_c	a_{tot}	a_{expt}	Tensor $axis_{theor}$	b_l	b_{tot}	b'	b_{expt}	b'_{expt}	Tensor $axis_{expt}$
$Al_i^{++}(0,0,0)$	1225	25	3.0	1253	±1180	[111]	0.29	0.31		±3.3		[111]
$Al_{Si}^{-}(1,1,1)$	33.5	−0.23	−0.56	32.7	±37.75	[111]	0.51	0.80		±1.1		[111]
$Si(1,\bar{1},\bar{1})$	−50.7	0.17	0.30	−50.2	±56.76	[1 $\bar{1}$ $\bar{1}$]−24°	−0.22	−0.32	0.07	∓0.41	∓0.18	[1 $\bar{1}$ $\bar{1}$]+12°
Si(2,0,0)	−39.4	−0.70	0.35	−39.75	±25.46	[100]−11°	−2.41	−2.44	0.03	±1.02	±0.18	[100]+5°
$Si(\bar{2},0,0)$	−36.4	1.0	—	−35.4	±24.41	[100]+1.9°	−2.01	−1.92	0.12	±1.42	∓0.23	[100]+7°
$Si(3,\bar{1},\bar{1})$	−0.13	0.52	—	0.39			−0.29					
Si(2,2,2)	−44.4	−2.3	0.6	−46.1	±31.32	[111]	−4.21	−4.14		±3.98		[111]
$Si(2,\bar{2},\bar{2})$	−51.8	0.35	—	−51.44	±60.76		−5.15			±6.08		
$Si(\bar{2},\bar{2},\bar{2})$	−12.1	0.1	—	−12.0	±13.53	[111]	−0.02	−0.08		±0.16		[111]
Si(3,3,1)	−0.17	0.60	—	0.43		[331]+63°	−0.36	−0.34	≃ 0			
$Si(\bar{3},\bar{3},1)$	− 0.98	0.02	—	−0.96			−0.54					

TABLE IV. Comparison of the calculated hyperfine data for the different trigonal $(Al_i\text{-}Al_{Si})^+$ defect pairs (in MHz) with the experimental HFI interactions at the ^{27}Al nuclei for Si-G19 taken from Watkins (Ref. 1).

	Al_i^{++}		Al_{Si}^-	
Pair	a	b	a	b
(a)	1253	0.31	32.74	0.80
(b)	1200	0.33	31.8	2.17
(c)	1300	0.66	10.95	0.07
(d)	1286	0.26	1.61	0.008
Si-G19	±1180	±3.31	±37.75	±1.1

embracing the experimental value. Pair (b) can however be discounted as a candidate for Si-G19 because the HFI interaction for the Si(1,1,1) ligand would be $a_{tot} = -11.6$ MHz and $b_{tot} = -2.4$ MHz according to our calculation which is not compatible with the experimental HFI data. The fact that this would be the only major discrepancy for pair (b) indicates strongly that the atomic structure of this pair is incorrect. We, therefore, conclude that we have an excellent agreement between theory and experiment if we identify pair (a) with Si-G19. Still the agreement is considerably less convincing than that found for the isolated interstitial Al_i^{++} point defect. In particular our calculated data underestimate systematically the subshell splitting of the HFI data. This might be due to a trigonal lattice distortion which is not included in our present calculation. This distortion, however, does not seem to have a major effect on the HFI data.

V. TRIGONAL Al_i-Al_{Si}-Al_{Si} AND Al_i-Al_{Si}-C_{Si} CLUSTERS

Since the paramagnetic properties of the trigonal pairs did not show the characteristic value $a_{expt} = 127$ MHz found by EPR for the HFI contact interaction *with* the Al_{Si} nucleus in the pair Si-G20 (Ref. 1) we have made an attempt to calculate the HFI data for larger trigonal clusters which besides the Al_i-Al_{Si} trigonal defect consist of additional ingredients. Following a suggestion of Watkins[4] we have tried C_{Si} besides Al_{Si} as additional members of the trigonal clusters. The structure of these clusters is sketched in Fig. 5.

We determine the cluster formation energy as the difference between the total energy for the cluster and the sum of the total energies for the $(Al_i^{++}\text{-}Al_{Si}^-)$ pair and for the additional constituent of the cluster. We find for the trigonal $(Al_i\text{-}Al_{Si}\text{-}Al_{Si})$ cluster (a) a very small formation energy of −0.1 eV as is to be expected for a $(Al_i^{++}\text{-}Al_{Si}^-)$ pair where an Al_{Si}^- defect is to be attached to the Al_{Si}^- side of the pair. In contrast the $(Al_i\text{-}Al_{Si}\text{-}Al_{Si})$ cluster (b) has

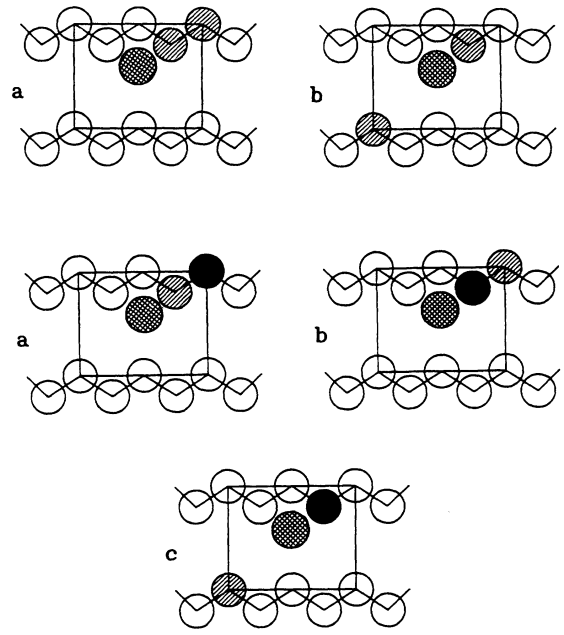

FIG. 5. Schematic representations of the different configurations of trigonal Al_i-Al_{Si}-Al_{Si} and Al_i-Al_{Si}-C_{Si} clusters in Si. Hatched balls represent Al_{Si}, cross line hatched circles represent Al_i, black circles represent C_{Si}, and plain circles represent Si atoms.

a binding energy of −0.9 eV—the distance between the $(Al_i\text{-}Al_{Si})^+$ pair and the additional Al_{Si}^- is larger but the positive charge is now surrounded by negative charges on both sides. We note that the formation of Al triplets may be promoted by the existence of divacancy centers which have been observed by Watkins and Corbett[16] and by Brower[2] in electron-irradiated Al-doped Si crystals. These might, e.g., trap the Al interstitials one-by-one during the annealing process.

The situation is different for the $(Al_i\text{-}Al_{Si}\text{-}C_{Si})$ clusters because here the additional C_{Si} atom is neutral and for the binding of the C_{Si} atom to the $(Al_i\text{-}Al_{Si})^+$ pair electrostatic effects play no role. We find for $(Al_i\text{-}Al_{Si}\text{-}C_{Si})$ cluster (a) and for $(Al_i\text{-}Al_{Si}\text{-}C_{Si})$ cluster (c) that the cluster formation energy is slightly positive with $E^{form} = 0.1$ eV [cluster (a)] and $E^{form} = 0.5$ eV [cluster (c)]. For $(Al_i\text{-}Al_{Si}\text{-}C_{Si})$ cluster (b), however, the formation energy with $E^{form} = -1.3$ eV seems to be unexpectedly high. This is, however, not quite correct because in this case we should calculate the cluster formation energy as the difference between the total energy for the cluster and the sum of the total energies for the $[Al_i(0,0,0)\text{-}C_{Si}(1,1,1)]$ pair and for an additional substitutional aluminum. Since for the $[Al_i(0,0,0)\text{-}C_{Si}(1,1,1)]$ pair the formation energy of −2 eV exceeds that for the $(Al_i\text{-}Al_{Si})$ pair (a) (−0.7 eV) we obtain a cluster formation energy which is also close to zero.

The HFI matrix elements for the interaction with the ^{27}Al and the ^{13}C nuclei (in parentheses) are listed in Table V. We find that the interaction matrix element with the ^{27}Al nucleus of the interstitial Al is not very much affected by the formation of the cluster while the inter-

TABLE V. Comparison of the calculated hyperfine data for the different trigonal $(Al_i\text{-}Al_{Si}\text{-}Al_{Si})^0$ and $(Al_i\text{-}Al_{Si}\text{-}C_{Si})^+$ defect clusters sketched in Fig. 5 (in MHz) with the experimental HFI interactions at the ^{27}Al nuclei for Si-G19 and for Si-G20 taken from Watkins (Ref. 1). The interactions with the ^{13}C nuclei are in parentheses.

Cluster	a	b	a	b	a	b
	$Al_i^{++}(0,0,0)$		$Al_{Si}^{-}(1,1,1)$		Al_{Si}	
$(Al_i\text{-}Al_{Si}\text{-}Al_{Si})^0$ cluster (a)	1042	2.8	2.7	3.4	42.5	5.6
$(Al_i\text{-}Al_{Si}\text{-}Al_{Si})^0$ cluster (b)	1257	1.3	40.0	0.05	12.6	2.3
	$Al_i^{++}(0,0,0)$		Al_{Si}^{-}		C_{Si}	
$(Al_i\text{-}Al_{Si}\text{-}C_{Si})^+$ cluster (a)	1185	0.9	56.2	0.05	(66.8)	(3.25)
$(Al_i\text{-}Al_{Si}\text{-}C_{Si})^+$ cluster (b)	1548	2.9	23.0	0.8	(112)	(1.6)
$(Al_i\text{-}Al_{Si}\text{-}C_{Si})^+$ cluster (c)	1169	3.2	40.3	0.8	(25.8)	(0.4)
Si-G19	±1180	±3.31	±37.75	±1.1		
Si-G20	±1162	±2.99	±127.0	±0.5		

action with the nucleus of the Al_{Si}^{-} atom for all clusters except $(Al_i\text{-}Al_{Si}\text{-}C_{Si})$ cluster (b) is somewhat enlarged. The case of $(Al_i\text{-}Al_{Si}\text{-}Al_{Si})$ cluster (a) is quite interesting because here the spin density is predominantly found in the $Al_i^{++}(0,0,0)$ and the $Al_{Si}^{-}(2,2,2)$ ASA spheres but remarkably little spin density at the intermediate $Al_{Si}^{-}(1,1,1)$ nucleus. One might speculate that a trigonal lattice relaxation could support this effect and lead to a pile-up of s-like spin density at the $Al_{Si}^{-}(2,2,2)$ ligand. At present we are unable to treat this case. We, therefore, have no defect cluster for which the contact HFI at an Al_{Si}^{-} nucleus is comparable to the value of 127 MHz found experimentally by Watkins[1] some 35 years ago.

VI. CONCLUSIONS

We have performed total-energy calculations for isolated Al point defects and trigonal Al-Al pairs. Substitutional Al point defects were found to be the stable defects; all other defect configurations are metastable at most. We have studied in particular the paramagnetic Al_i^{++} impurity which has a deep level in the fundamental band gap. This state is well localized and more than 50% of the total spin density is shared by the impurity and its 14 nearest Si ligands. We have compared the calculated HFI data with EPR data reported by Watkins,[1] Brower,[2] and Niklas, Spaeth, and Watkins[3] for the defect Si-G18 identified by Watkins as Al_i^{++}. We find that the assignment of the experimental HFI data to the Si(1,1,1) and Si(2,2,2) shells has to be interchanged in order to be compatible with our results. We then find a close agreement of the calculated and experimental HFI data, both for the contact term and for the dipolar terms for which we give the full tensor.

No stable substitutional Al-Al pairs have been found and also the pairs of two interstitial Al atoms have at best a questionable stability against dissociation. We did find, however, mixed interstitial-substitutional pairs of trigonal symmetry to be stable with respect to dissociation. Of particular stability is the pair where the substitutional Al defect atom is situated next to a tetrahedral interstitial Al atom. For this pair we find a striking similarity of the calculated HFI data with the experimental data reported by Watkins,[1] and Niklas, Spaeth, and Watkins[3] for the defect Si-G19 if a similar interchange of the assignments as above is made for the $Si(1,\bar{1},\bar{1})$ and the $Si(2,\bar{2},\bar{2})$ shells.

None of the pairs shows the large contact HFI at the Al_{Si} atom which is characteristic for the trigonal Si-G20 defect which is known[1] to contain Al_i and at least one Al_{Si} defect atom. We have calculated the total energies and magnetic properties of trigonal clusters that in addition contained an extra Al_{Si} or C_{Si}. We did find clusters that are stable against dissociation and we also found that the contact HFI interaction at the $^{27}Al_{Si}$ nuclei could be nearly a factor of 2 larger than for the pairs. We did not find, however, a cluster for which the contact HFI at the Al atom was comparable to the experimental value of 127 MHz which is more than a factor of 2 above the highest value found in our clusters. Clusters which involve vacancies seem to be interesting candidates for Si-G20 and preliminary calculations have resulted in interesting results which will be reported in a subsequent paper.

ACKNOWLEDGMENTS

One of us (G.C.) is grateful to the Theoretical Physics group of the University of Paderborn for the kind hospitality during his stay in Paderborn. Financial support from the Deutsche Forschungsgemeinschaft and the National Scientific and Research Fund (OTKA) of Hungary is thankfully acknowledged.

[1] G. D. Watkins, in *Radiation Damage in Semiconductors*, edited by P. Baruch (Academic, New York, 1965), p. 97.
[2] K. L. Brower, Phys. Rev. B **1**, 1908 (1970).
[3] J. R. Niklas, J.-M. Spaeth, and G. D. Watkins, in *Microscopic Identification of Electronic Defects in Semiconductors*, edited by N. M. Johnson, S. G. Bishop, and G. D. Watson, MRS Symposia Proceedings No. 46 (Materials Research Society, Pittsburgh, 1985), p. 237.
[4] G. D. Watkins (private communication).
[5] O. Gunnarsson, O. Jepsen, and O. K. Andersen, Phys. Rev. B **27**, 7144 (1983).
[6] H. Overhof, M. Scheffler, and C. M. Weinert, Mater. Sci. Forum **38-41**, 293 (1989).
[7] H. Overhof, M. Scheffler, and C. M. Weinert, Mat. Sci. Eng. **4**, 315 (1989).
[8] H. Overhof, M. Scheffler, and C. M. Weinert, Phys. Rev. B **43**, 12 494 (1991).
[9] F. Beeler, M. Scheffler, O. Jepsen, and O. Gunnarsson, Phys. Rev. Lett. **54**, 2525 (1985).
[10] F. Beeler, O. K. Anderson, and M. Scheffler, Phys. Rev. B **41**, 1603 (1990).
[11] H. Overhof and G. Corradi, Mater. Sci. Forum **83-87**, 279 (1991).
[12] J. R. Troxell, A. P. Chatterjee, G. D. Watkins, and L. C. Kimerling, Phys. Rev. B **19**, 5336 (1979).
[13] D. A. van Wezep, T. Gregorkiewicz, E. G. Sieverts, and C. A. J. Ammerlaan, Phys. Rev. B **34**, 4511 (1986).
[14] S. Greulich-Weber, A. Görger, J.-M. Spaeth, and H. Overhof, Appl. Phys. A **53**, 147 (1991).
[15] M. Lannoo, in *Submicroscopic Studies of Defects in Semiconductors*, edited by G. Langouche (North-Holland, Amsterdam, in press).
[16] G. D. Watkins and J. W. Corbett, Phys. Rev. **138**, A543 (1965).